Electronic Supplementary Material (ESI) for Nanoscale.
This journal is © The Royal Society of Chemistry 2014

Structural characterisation of a layered double hydroxide nanosheet

SUPPLEMENTARY INFORMATION

Nicholas P Funnell,[a] Qiang Wang,[a,b] Leigh Connor,[c] Matthew G Tucker,[c,d]
Dermot O'Hare[a,*] and Andrew L Goodwin[a,*]

[a] Department of Chemistry, University of Oxford, Inorganic Chemistry Laboratory,
South Parks Road, Oxford, OX1 3QR, UK
[b] College of Environmental Science and Engineering, Beijing Forestry University, 35 Qinghua East Road,
Haidan District, Beijing 100083, China
[c] Diamond Light Source, Harwell Science and Innovation Campus, Fermi Avenue,
Didcot, OX11 0QX, UK
[d] ISIS Facility, Rutherford Appleton Laboratory, Harwell Science and Innovation Campus,
Didcot, OX11 0QX, UK
[*]To whom correspondence should be addressed;
E-mail: dermot.ohare@chem.ox.ac.uk; andrew.goodwin@chem.ox.ac.uk.

Submitted to Nanoscale

Contents

1 RMCProfile refinement of a two-dimensional material 3

2 Total scattering structure factor 5

3 A nanosheet LDH pair distribution function 6

4 Instantaneous and average structures 8

5 Geometric restraints applied during RMC refinement 10

6 Cation ordering signature in reciprocal space 11

7 References 12

1 RMCProfile refinement of a two-dimensional material

The RMC configuration contains a single two-dimensional sheet from which the individual pair correlation functions g_{ij}^{RMC} are calculated. The meaning of this term is given by

$$g_{ij}^{\text{RMC}} = \frac{n_{ij}^{\text{RMC}}(r)}{4\pi r^2 \mathrm{d}r c_j \rho_{\text{RMC}}}, \tag{1}$$

where $n_{ij}^{\text{RMC}}(r)$ is simply the number of particles of type j at distances between r and $r + \mathrm{d}r$ from a particle of type i in the RMC configuration, and c_j is the relative concentration of particles of type j.[S1] These pair correlation functions are combined to produce the $D(r)$ function actually calculated by RMCProfile:

$$D_{\text{RMC}}(r) = 4\pi r \rho_{\text{RMC}} \sum_{i,j} c_i c_j f_i f_j [g_{ij}^{\text{RMC}}(r) - 1]. \tag{2}$$

This function is somewhat arbitrary since the RMC number density ρ_{RMC} is artificially set by the user as described in the text (recalling most of the RMC box is void space). What we are after is the 'real' $D(r)$ function, given by

$$D(r) = 4\pi r \rho \sum_{i,j} c_i c_j f_i f_j [g_{ij}(r) - 1], \tag{3}$$

where

$$g_{ij} = \frac{n_{ij}(r)}{4\pi r^2 \mathrm{d}r c_j \rho}. \tag{4}$$

We proceed by considering two separate cases for pairs of atoms i, j: case 1 is for pairs separated by distances less then half the layer width $d/2$; case 2 is for pairs separated by distances greater than this value. In case 1, we can be sure that the atoms are within the same layer and hence the corresponding term $n_{ij}(r)$ is actually the same as that determined in the RMC refinement: *i.e.*, $n_{ij}(r) = n_{ij}^{\text{RMC}}(r)$ and so

$$g_{ij}(r) = \frac{\rho_{\text{RMC}}}{\rho} g_{ij}^{\text{RMC}}(r). \tag{5}$$

In case 2 there is some probability that the pair of atoms chosen do not lie within the same sheet, in which case $g_{ij}(r) \equiv 1$ (*i.e.*, they are considered completely uncorrelated). This probability is related to the volume of the annulus of radius r and width d relative to the volume of the spherical shell of radius r [Fig. S1] and is easily shown to equal $1 - d/2r$. Consequently in case 2 one has

$$g_{ij}(r) = \frac{\rho_{\text{RMC}}}{\rho} g_{ij}^{\text{RMC}}(r) + \left[1 - \frac{d}{2r}\right], \tag{6}$$

where the first term on the right-hand side accounts for the correlated pairs within the nanosheet (of which there are $n_{ij}(r) = n_{ij}^{\text{RMC}}(r)$, as for case 1 above) and the second term accounts for the uncorrelated pairs between different nanosheets.

Combining equations (3), (5) and (6), we obtain

$$D(r) = D_{\text{RMC}}(r) + 4\pi r \delta(r) \rho \sum_{i,j} c_i c_j f_i f_j \left[\frac{\rho_{\text{RMC}}}{\rho} - \frac{d}{2r}\right], \tag{7}$$

where $\delta(r)$ is equal to zero for $r < d/2$ and equal to unity for $r \geq d/2$ (and essentially distinguishes cases 1 and 2).

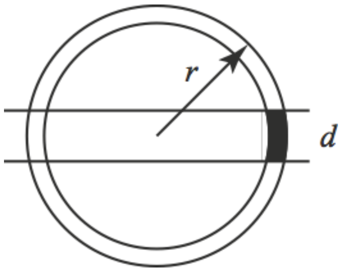

Figure S1: Derivation of the fraction of correlated and uncorrelated pairs of atoms in a nanosheet sample at separation r and sheet thickness d. The total number of pairs of atoms i, j separated by distances between r and $r + \mathrm{d}r$ is proportional to the volume of the corresponding spherical shell: $V_{\text{shell}} = 4\pi r^2 \mathrm{d}r$. The number of pairs of atoms i, j separated by the same distances but *within the same nanosheet* is proportional to the volume of an annulus of the same diameter r and thickness d: $V_{\text{annulus}} = 2\pi r d \mathrm{d}r$. Consequently the fraction of pairs of atoms i, j within the same nanosheet is given by $V_{\text{annulus}}/V_{\text{shell}} = d/2r$ and hence the fraction that is uncorrelated is given by $1 - d/2r$.

2 Total scattering structure factor

The total scattering data were measured to a maximum scattering vector of 33 Å^{-1}, however these data were truncated at 17 Å^{-1} owing to unfavourable signal-to-noise ratios at higher magnitudes of Q; most likely a result of form-factor falloff. The $F(Q)$ data, plotted against the full measured Q-range, and at 30 Å^{-1} (for clarity) are given below. The data shown have not been degraded by convolution with the RMC box dimensions and thus appear 'cleaner' than those data shown in the main manuscript, lacking the spurious ripples arising from Fourier transform over finite limits.

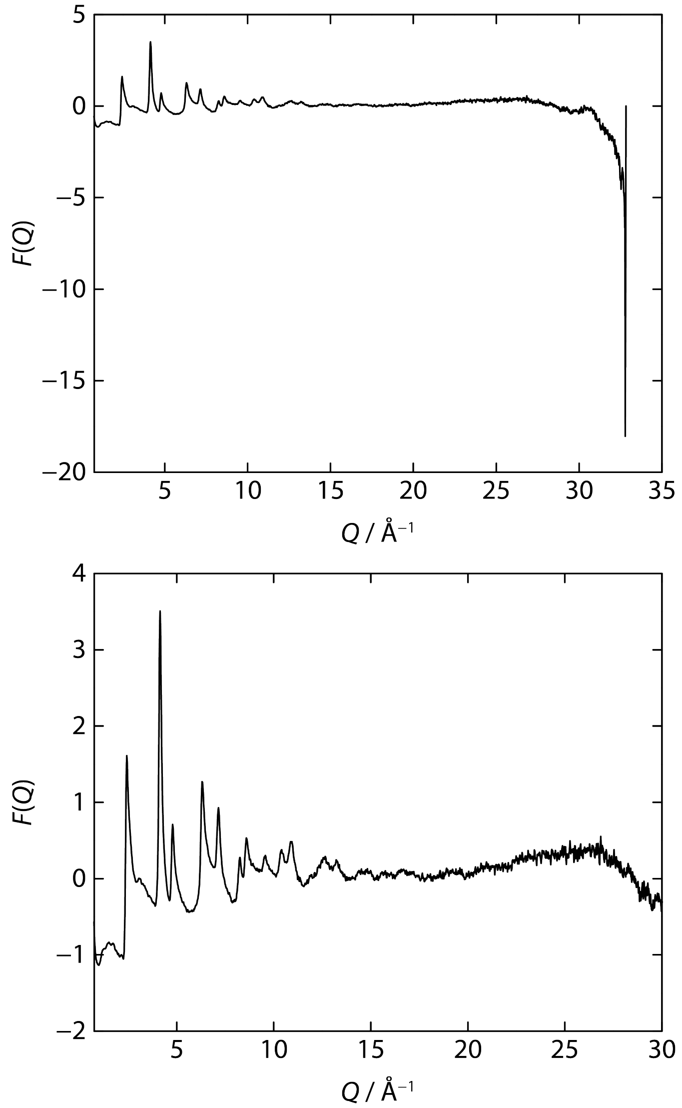

Figure S2: $F(Q)$ data shown against the full measured Q range (top) and also to 30 Å^{-1} (bottom) for clarity.

3 A nanosheet LDH pair distribution function

The measured and RMC-refined pair distribution functions for the LDH nanosheet are reproduced from the main manuscript in Figure S2. While it is evident that the RMC-refined PDF captures the qualitative features of the experimental pattern, there are quantitative discrepancies, particularly at very low r ($<$5 Å) where relatively strong 1,2 and 1,3 interactions dominate.

At low-r, the under-fitted peaks can be attributed broadly to the absence of borate counter-ions in the RMC model. Although each LDH nanosheet is coated with borate anions, preserving charge neutrality, their spatial positions are unlikely to be well-defined and, as a direct consequence, will not show any significant correlations over greater length scales than those of the molecules themselves. This, coupled with the inherent difficulty in modelling molecular species[S2, S3], led to the decision not to include the borate counter-ions as part of an already-challenging refinement.

An unfitted peak at 1.4 Å can be ascribed solely to the B–O bond but contributions from 1,3–1,5 intramolecular interactions can account easily for additional under-fitted peak intensity. Assessment of bond distances in a tetraborate structure, deposited in the Cambridge Structural Database[S4] (refcode: BOJWIG10) reveals 1,3 interactions fall within the ranges 2.350–2.431 and 2.427–2.480 Å for O–(B)–O and B–(O)–B, respectively. Higher-order correlations (1,4 and 1,5) between B–O and B–B/O–O atoms make additional contributions to intensity continuously between 2.720–3.736 and 4.632–4.771 Å. Analysis of a triborate structure (refcode: SIZFUD) shows that comparable intraatomic distances are present here also. However, the PDF data presented here are sensitive to fluctuations in the average structure and so the real range of intraatomic distances is likely to be even broader than those described above, contributing effectively to all low-r peaks.

At high-r ($>$15 Å), the data are over-fitted by the model suggesting incorrectly the existence of stronger long-range correlations. This is most likely due to instrumental resolution in reciprocal space ΔQ that can lead to damping at high r.

An added complication is determination of the initial slope on the fitted data, owing to the difficulty both in measurement of the bulk LDH density and defining what constitutes ‘density’ in a loosely-aggregated nanosheet system. The over-intense baseline of the fitted PDF is evidence of an imperfect value used for the sample density in data normalisation.

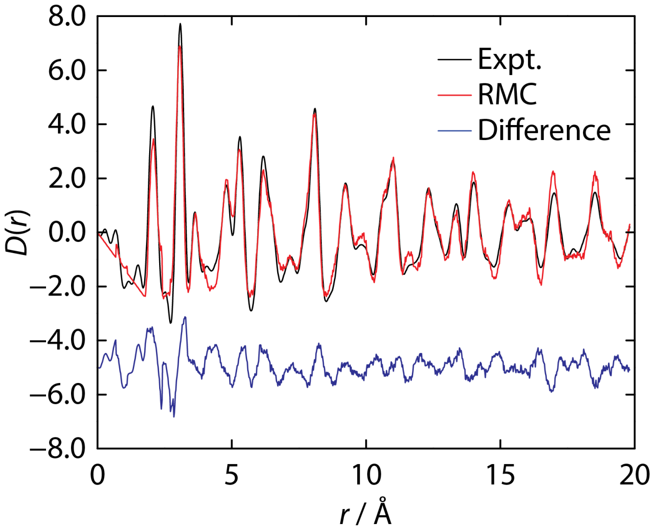

Figure S3: Measured (black) and RMC-refined (red) pair distribution function for the nanosheet LDH. The difference curve is shown in blue.

4 Instantaneous and average structures

The geometric analyses, given in Tables S1 and S2, have been derived from two subtly different interpretations of the RMC-refined model, hereafter referred to as being ‘instantaneous’ and ‘average’. In both cases, the atoms in the respective supercells have first been collapsed back down onto the equivalent positions in a single ‘unit cell’, with periodicity in two-dimensions only. The values reported for the instantaneous model refer to the average distance, or angle, between instantaneous atomic positions where the error is simply the standard deviation of all values. In the average model (shown in Figure 3 in the main manuscript), the distances and angles reported are those between average coordinates — analogous to the structure that would typically be obtained by a conventional Rietveld refinement. From the distribution of atomic positions, we are able to calculate anisotropic displacement parameters (ADPs), constrained by $P\bar{3}m1$ layer symmetry, the eigenvalues of which are given in Table S2. Hydrogen atoms have been omitted from Tables S1 and S2, owing to a very large uncertainty in their spatial distribution.

A notable difference between the models is the occurrence of shorter metal–oxygen bond lengths in the average structure. The origin of this discrepancy is described in more detail elsewhere[S5], but outlined briefly here: the effect of taking the average atomic position of two atoms is to move the centre of mass closer to the (more) stationary atom, giving the appearance of a shorter bond. Thus calculation of the *average* distance between *instantaneous* atomic coordinates provides a more accurate depiction of bond lengths than does the distance between *average* atomic coordinates.

Table S1: Instantaneous and average bonding geometries

Bond/angle	Instantaneous (Å / °)	Average (Å / °)
Al–O	2.15(16)	2.092(8)
Zn–O	2.16(14)	2.092(8)
O–Al–O	90(6)	86.2(8)
O–Zn–O	90(6)	86.2(8)
Al–O–Al	90(6)	93.8(8)
Zn–O–Zn	93(5)	93.8(8)
Al–O–Zn	92(5)	93.(8)

Estimated standard errors are given in parentheses.

Table S2: Averaged atomic coordinates and anisotropic displacement parameters, derived from the RMC-refined model

a (Å)	3.054(17)	
Layer group	$P\bar{3}m1$	
Parameter	Al/Zn	O
x	0	$\frac{2}{3}$
y	0	$\frac{1}{3}$
z (Å)	0	1.1251(27)
U_{11} (Å^2)	0.01490	0.02862
U_{22} (Å^2)	0.01490	0.02862
U_{33} (Å^2)	0.00604	0.00671
U_{12} (Å^2)	0.00745	0.06712
U_{23} (Å^2)	0	0
U_{13} (Å^2)	0	0

Estimated standard errors are given in parentheses.

5 Geometric restraints applied during RMC refinement

Briefly discussed in the main manuscript was the need to apply soft bond length and angle restraints in order to maintain chemically sensible connectivity; without this information, RMCProfile can generate models with implausible geometry. Bond distance and angle restraints were applied in the form of molecular mechanics potentials, the parameters for which are given in Table S3. In the absence of suitable quantitative *ab initio* values to guide choice of different effective spring constants for the different terms, we have used the default RMCProfile values. It has been shown elsewhere that, for suitable choice of the weighting of the soft restraints (relative to the data) during RMC refinements, the absolute magnitude of the effective spring constant has negligible effect on the resulting structural model.[S6]

Table S3: RMCProfile potentials used

Bond/angle	Restraint value (Å / °)	Energy (eV)
Al–O	2.07	2.544
Zn–O	2.07	2.544
H–O	0.85	3.662
H–O–Al	120.0	3.121
H–O–Zn	120.0	3.121
O–Al–O	90.0	7.490
O–Al–O	180.0	7.490
O–Zn–O	90.0	7.490
O–Zn–O	180.0	7.490
Al–O–Al	98.0	3.121
Zn–O–Zn	98.0	3.121
Zn–O–Al	98.0	3.121

6 Cation ordering signature in reciprocal space

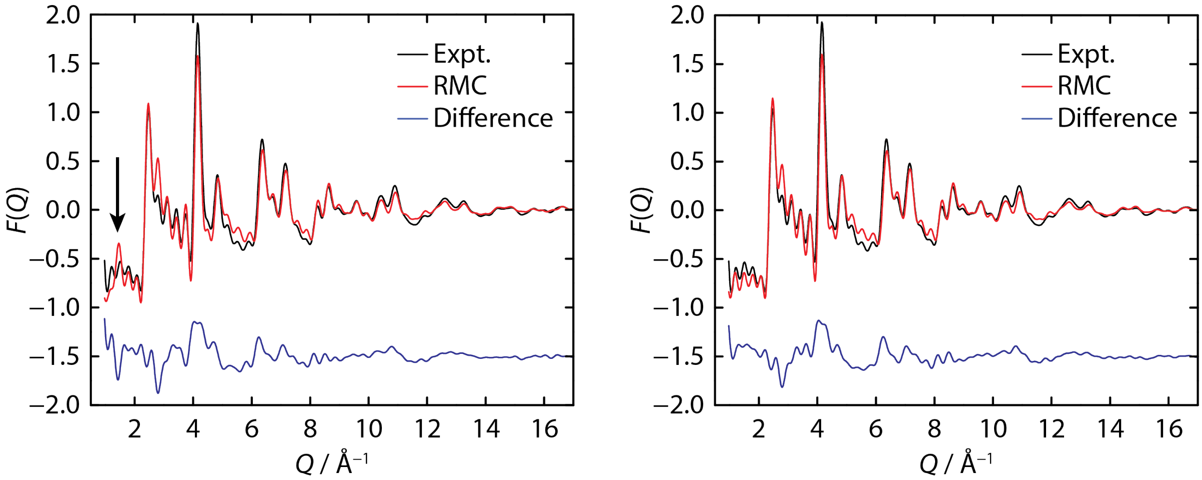

Figure S4: RMC fit to $F(Q)$ data with an ordered cation configuration ($n_{\mathrm{Al}}^{\mathrm{Al}} = 0$), left and disordered, right. The strongest signature of cation ordering is present in the form of a peak at *ca.* 1.8 $\mathrm{\AA}^{-1}$ in the RMC model, indicated by an arrow in the left-hand plot

7 References

(S1) D. A. Keen, *J. Appl. Cryst.* **34**, 172 (2001).

(S2) N. P. Funnell, M. T. Dove, A. L. Goodwin, S. Parsons, M. G. Tucker, *J. Phys.: Condens. Matter* **25**, 454201 (2013).

(S3) N. Rademacher, L. Daemen, E. Chronister, T. Proffen, *J. Appl. Cryst.* **45**, 482 (2012).

(S4) F. H. Allen, *Acta Cryst.* **B58**, 380 (2002).

(S5) M. Dove, M. Tucker, D. Keen, *Eur. J. Mineral.* **14**, 331 (2002).

(S6) M. G. Tucker, D. A. Keen, M. T. Dove, A. L. Goodwin, Q. Hui, *J. Phys.: Condens. Matter* **19**, 335218 (2007).